THE ASTROPHYSICAL JOURNAL, 449:L119–L122, 1995 August 20

THE FIRST 8–13 MICRON SPECTRA OF ASYMPTOTIC GIANT BRANCH STARS IN THE MAGELLANIC CLOUDS

M. A. T. GROENEWEGEN
Institut d'Astrophysique de Paris, CNRS, 98 bis Boulevard Arago, F-75014 Paris, France
C. H. SMITH
Department of Physics, University College, ADFA, Canberra ACT 2600, Australia
P. R. WOOD
Mount Stromlo and Siding Springs Observatories, Private Bag, Weston Creek P.O., Canberra ACT 2611, Australia
A. OMONT
Institut d'Astrophysique de Paris, CNRS, 98 bis Boulevard Arago, F-75014 Paris, France
AND
T. FUJIYOSHI
Department of Physics, University College, ADFA, Canberra ACT 2600, Australia
Received 1995 May 15; accepted 1995 June 8

ABSTRACT

We have obtained 8–13 μm spectra of two asymptotic giant branch stars in the Magellanic Clouds (MCs) and report the first detection of dust features in AGB stars in the MCs. The long-period variable (LPV) TRM 60 (P = 1260 days) in the LMC displays silicate absorption, and the LPV GM 103 (P = 1070 days) in the SMC shows silicate emission. The presence of silicates confirms previous observations using different techniques that these stars are oxygen rich. By modeling the spectral energy distributions and 8–13 μm spectra with a dust radiative transfer model we find that although the two stars have similar high luminosities their dust optical depths differ by a factor of 10.

A similar analysis was carried out for a Galactic OH/IR star of comparable period. The results for these three stars suggest that the mass-loss rate increases with metallicity in AGB stars.

Subject headings: circumstellar matter — stars: AGB and post-AGB — stars: mass loss — infrared: stars

1. INTRODUCTION

Searches for asymptotic giant branch (AGB) stars in the Magellanic Clouds (MCs) have been made using optical spectroscopic surveys (see, e.g., Blanco, McCarthy, & Blanco 1980; Blanco & McCarthy 1991; Rebeirot, Azzopardi, & Westerlund 1991), photometric surveys using V and I Schmidt plates (see, e.g., Reid, Mould, & Thompson 1987), and optical surveys for LPVs (see, e.g., Payne-Gaposhkin 1971; Hughes 1989). However, these surveys failed to identify the red dust-enshrouded OH/IR stars and infrared carbon stars in the MCs, very luminous examples of which did turn up in the *IRAS* point source catalog. Recently, near-infrared studies have been initiated to study *IRAS* sources in the MCs (Reid, Tinney, & Mould 1990; Reid 1991; Wood et al. 1992 [hereafter W92]; Zijlstra et al. 1995). From NIR data alone it is almost impossible to distinguish between an oxygen- and a carbon-rich dust enshrouded object. To determine the chemical type of obscured stars one can use narrowband 10 μm photometry (Zijlstra et al. 1995) or look for OH emission (e.g., W92). A direct way is to observe the 8–13 μm region and look for the 9.8 μm silicate or 11.3 μm silicon carbide dust feature.

Here we report on the detection of the silicate dust feature in one LMC and in one SMC AGB star. We model the spectral energy distributions (SEDs) and 8–13 μm spectra and determine the luminosity and (dust) mass-loss rate.

2. OBSERVATIONS

The data were taken on 1994 November 25–27 with the UCL IR cooled grating array spectrometer (for details see Aitken & Roche 1982) mounted at the f/36 Cassegrain focus of the 3.9 m Anglo-Australian Telescope. We used a circular aperture of 4″.2 diameter, while the (optical) seeing was in the range 1″.0–1″.5 for most of the time. The 8.0–13.0 μm window was covered with 25 detectors, resulting in an effective resolution of $\lambda/\Delta\lambda \approx 50$. The grating was stepped once, offset by one and a half detector widths, providing an oversampled (50 data point) spectrum, which was subsequently smoothed. Chopping, with a frequency of 12.5 Hz, and beam switching were employed, each using a throw of 15″ in declination. The pointing of the telescope was regularly verified on a bright nearby star. The observations were obtained through cirrus clouds which is reflected by the large error bars. Flux calibration and correction for telluric absorption were made by reference to the F0II star α Car.

We observed nine objects but detected only TRM 60 (IRAS 05529−6708) and GM 103 (see Table 1). The nondetection of the others is most likely due to variability since it turns out that the two stars detected were observed near maximum light.

The spectra of TRM 60 and GM 103 are shown in Figures 1 and 2. The on-source integration times are 21.3 and 32 minutes, respectively. The spectrum of GM 103 clearly indicates silicate emission, while that of TRM 60 possibly suggests silicate absorption, although the S/N is poor.

3. MODELING

Since both stars are long-period variables (LPVs) it is important to use photometry taken as close as possible in phase to the AAT observations. Based on the periods and the

TABLE 1

OBSERVED PARAMETERS

Name	Period (days)	Position (1950)	J	H	K	L'	S_{12} (Jy)	S_{25} (Jy)
TRM 60	1260	$5^h32^m55\overset{s}{.}2$ $-67°08'49''$	14.90 ± 0.30	11.66 ± 0.17	9.48 ± 0.20	7.18 ± 0.26	1.09	1.59
GM 103	1070	0 48 44.1 −73 07 50	10.11 ± 0.10	9.10 ± 0.15	8.57 ± 0.20	...	0.44	0.89

time of maximum light (W92; Wood, Moore, & Bessell 1995 [hereafter W95]) the AAT observations of TRM 60 are obtained at phase 0.13 and those of GM 103 at phase 0.95. From W92 for TRM 60 and W95 for GM 103 we took *JHK*(*L'*) photometry closest in phase to the AAT observations. The magnitudes are listed in Table 1 which include "error bars" indicating the change in magnitudes over ~0.05 in phase from the adopted photometry. In addition, we list the *IRAS* 12 and 25 μm flux-densities from the *IRAS* Faint Source Catalog (hereafter FSC; TRM 60) and Schwering & Israel (1989; GM 103). The SEDs and 8–13 μm spectra were modeled using the model of Groenewegen (1993 chap. 5) assuming a r^{-2} density distribution. For the central star the theoretical model flux of a M4 star is used (Fluks et al. 1994; $T_{\rm eff}$ = 3490 K). Changing the flux from an M4 star to that of a 2500 K blackbody does not change the results significantly; the effects are largest for GM 103 which has a lower mass-loss rate (see Table 2). The silicate dust opacity of Volk & Kwok (1988; hereafter VK) and a combination of dirty silicate (Jones & Merrill 1976) and the silicate feature of David & Papoular (1990), hereafter JMDP) are used. The inner dust radius is determined by imposing a condensation temperature of the dust of T_c = 1000 K. Luminosities are determined by adopting a distance to the LMC of 50 kpc, and to the SMC of 60 kpc. A foreground extinction of A_V = 0.1 is assumed.

The best fits are shown in Figures 1 and 2 with model parameters listed in Table 2. We recall that the fitting process only fixes the dust optical depth, which is related to physical parameters in the present model by $\tau_\lambda \sim (\dot{M}\Psi\kappa_\lambda)/(R_* r_{\rm inner} v)$, where $\dot{M}$ is the total mass-loss rate; Ψ, the dust-to-gas ratio; κ_λ, the dust opacity; R_*, the stellar radius in solar radii; $r_{\rm inner}$, the inner dust radius in stellar radii; and v the expansion velocity of the envelope.

The SEDs and mid-IR spectra are fitted well in general. For TRM 60 the VK dust gives an overall better fit to the SED. For GM 103, the VK dust gives a better fit to the 8–13 μm spectra if the models are scaled to the continuum. From the fit to GM 103 it is obvious that the *IRAS* 25 μm point (0.89 Jy) lies well above the predicted model flux-density (0.31–0.38 Jy). We inspected two-dimensional images and one-dimensional co-adds of *IRAS* scans using the GIPSY software package (Wesselius et al. 1992). At 25 μm, the one-dimensional co-add clearly indicates the source is not a point source. It is not clear, however, whether the source is physically extended. The *IRAS* image shows that there are two very red, strong 25 μm emitters (00489−7305 and 00478−7305) at less than 5'.2 from GM 103. Since the size of the 25 μm detector on the sky is 0'.75 × 4'.7 it is likely that emission from one or both of these nearby sources contaminates the published 25 μm flux of GM 103. We also find that GM 103 is a point source at 12 μm, as is TRM 60 at 12 and 25 μm.

We derive luminosities at the time of observation of ~55,000 and 80,000 $L_\odot$ for TRM 60 and GM 103, respectively, above the classical upper limit of ~54,000 $L_\odot$ ($M_{\rm bol}$ = −7.1), raising the question on the AGB character of the two stars. However, both stars are observed close to maximum light and based on published photometry (W92; W95) and model fitting we estimate mean luminosities of 46,500 and 51,000 $L_\odot$ for TRM 60 and GM 103, respectively, within the range expected for massive AGB stars. In addition, TRM 60 and GM 103 are

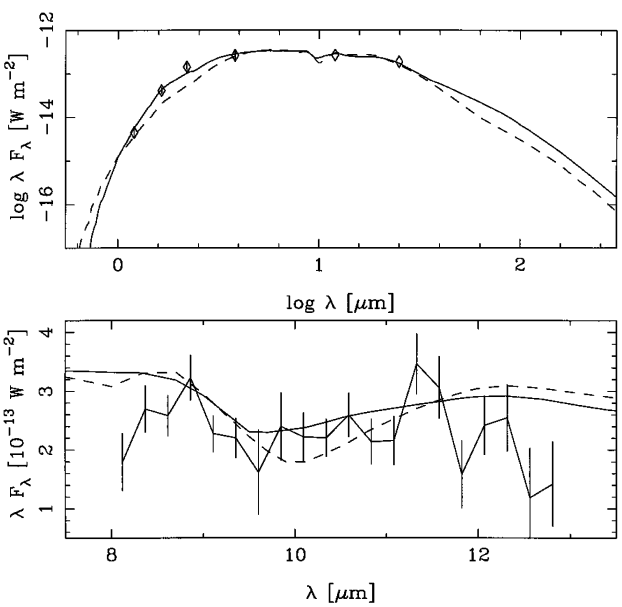

FIG. 1.—TRM 60. The solid line represents the best-fitting model with VK dust, the dashed line that with JMDP dust. The observed broadband photometry and *IRAS* fluxes are indicated by the diamonds.

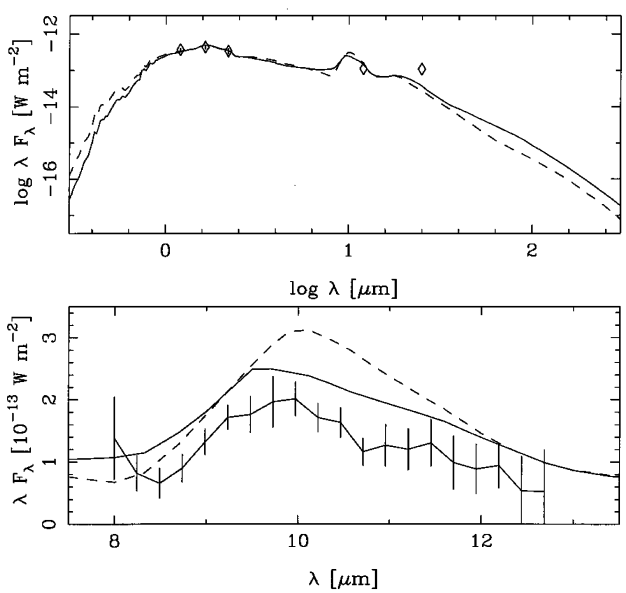

FIG. 2.—Same as Fig. 1 for GM 103

TABLE 2

MODEL RESULTS

Name (1)	Dust[a] (2)	Star[b] (3)	Luminosity ($L_\odot$) (4)	$\tau_{9.X}$[c] (5)	$\tau_{0.5}$[d] (6)	$\dot{M}$[e] ($M_\odot$ yr^{-1}) (7)
TRM 60.....	VK	M4	58000	4.1	18.2	$1.1\ 10^{-5}$
	JMDP	M4	54000	7.6	11.9	$6.0\ 10^{-5}$
	VK	BB	55000	4.2	18.7	$1.0\ 10^{-5}$
	JMDP	BB	55000	7.8	12.2	$5.8\ 10^{-5}$
GM 103	VK	M4	81000	0.44	1.93	$3.3\ 10^{-6}$
	JMDP	M4	84000	0.74	1.16	$1.8\ 10^{-5}$
	VK	BB	81000	0.20	0.87	$1.3\ 10^{-6}$
	JMDP	BB	76000	0.36	0.56	$7.0\ 10^{-6}$
OH 138	VK	M4	2160[f]	6.4	28.3	$2.0\ 10^{-6}$[g]
	JMDP	M4	2040[f]	7.9	12.4	$7.3\ 10^{-6}$[g]
	JMDP	M4	870[f]	12.2	19.1	$8.0\ 10^{-6}$[g]

[a] VK = Volk & Kwok 1988. JMDP is a combination of dirty silicate (Jones & Merrill 1976), and the silicate feature of David & Papoular 1990.

[b] The flux of the central star is either the flux of a M4 star with an effective temperature of 3490 K or a 2500 K blackbody.

[c] Optical depth at the peak of the silicate feature which occurs at 9.7 μm for VK dust and at 9.9 μm for JMDP dust.

[d] Dust optical depth at 0.5 μm.

[e] Total mass-loss rate, calculated from the optical depth, assuming a dust-to-gas ratio of $\Psi = 0.003$ (TRM 60), 0.001 (GM 103), 0.004 (OH 138) and $v = 12$ km s^{-1} (TRM 60, GM 103) or 9.4 km s^{-1} (OH 138; see Herman & Habing 1985).

[f] Luminosity ($L_\odot$)/[distance (kpc)]^2

[g] Mass-loss rate/distance ($M_\odot$ yr^{-1} kpc^{-1})

large-amplitude variables ($\Delta K = 1.9$ and 1.5 mag, respectively) which are not observed among supergiants (Wood et al. 1983).

In column (7) of Table 2 we list the mass-loss rate, assuming $v = 12$ km s^{-1} and a dust-to-gas ratio of $\Psi = 0.003$ (TRM 60) and 0.001 (GM 103). The expansion velocity of 12 km s^{-1} for TRM 60 is determined from the OH line profile (W92); for GM 103 we simply assume the same value, although one may expect a lower value. That the two types of silicates give so different mass-loss rates (for fixed v and Ψ) is due to the difference in dust opacity: $\kappa_{60} = 1910$ cm^2 g^{-1} for VK dust and 134 cm^2 g^{-1} for JMDP dust. The value for VK dust is significantly larger than usually quoted for silicate dust (150 cm^2 g^{-1}; Jura 1986, or 108 cm^2 g^{-1}; Schutte & Tielens 1989).

Independent of the uncertainty in v, Ψ or κ_λ the major conclusion of the model fitting is that a LMC and a SMC AGB star of comparable luminosity and pulsation period differ in dust optical depth by a factor of 10. This result is consistent with the observation of Wood et al. (1992) that the SMC contains two known luminous AGB stars with P > 1000 days and both are optically visible, while all known stars of this type in the LMC are deeply dust enshrouded and optically invisible.

4. DISCUSSION AND CONCLUSIONS

The detection of the silicate feature classifies TRM 60 and GM 103 as being oxygen-rich, and it demonstrates the usefulness of 8–13 μm spectroscopy as a tool to classify AGB stars. For both stars the oxygen-rich character was determined previously by other means. W95 detected TiO bands in an optical spectrum of GM 103, while W92 detected OH maser emission in TRM 60.

As TRM 60 and GM 103 have roughly the same period and luminosity but very different dust optical depths, the question arises if this is due to a difference in metallicity. In order to make the comparison we selected an oxygen-rich Mira in the

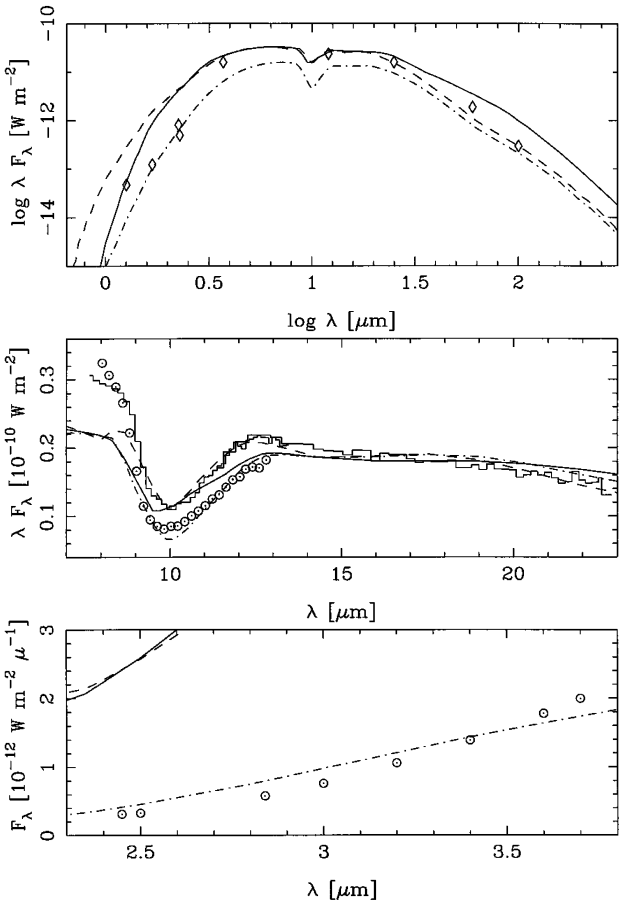

FIG. 3.—OH138+7.3. The solid line represents the best model with VK-dust, the dashed line that with JMDP dust, fitted to the *IRAS* data. The observed broadband photometry and *IRAS* fluxes are indicated by diamonds. The 2–4 and 8–13 μm spectra (*circles*) are from Smith & Herman (1990). The plotted 8–13 μm spectrum is the observed one multiplied by 4.5. Since the 2.4–2.5 and 2.8–3.7 μm spectra are featureless only the start and end, and some intermediate points are plotted. The dot-dashed line is the best model fitted to the 2–4 μm spectrum with JMPD dust. In the middle panel all models are scaled to the observed LRS spectrum near 15 μm.

Galaxy, the OH/IR star 138.0+7.3 (= IRAS 03206+6521; short OH 138) with a period of 1276 days (van Langevelde, Van der Heiden, & Schooneveld 1990) comparable to those of TRM 60 and GM 103. Broadband photometry was taken from Noguchi et al. (1993) and Jiang & Hu (1992). In addition, Smith & Herman (1990) presented near-simultaneous 8–13 and 2.8–3.6 μm spectra. The SED and LRS spectrum of this star are fitted in the same way as the MC stars. Interstellar extinction of $A_V = 3.0$ is adopted, based on Neckel & Klare (1980) and Burstein & Heiles (1982). The best-fitting models are presented in Figure 3 with parameters listed in Table 2.

In contrast to the two MC stars, the best fit to both the SED and the LRS spectrum (in particular, the location of the minimum at 10 μm) is obtained with JMDP dust. This may hint to a different type of silicate dust in the MCs possibly related to a different chemical composition.

From a comparison of three stars of comparable pulsation period in the (outer) Galaxy, the LMC, and the SMC, we derive that the dust optical depths have ratios of Galaxy : LMC : SMC $\approx$ 15 : 10 : 1. This is in all likelihood due to a difference in metallicity. If we assume that $\Psi \sim Z$ (the dust-to-gas ratio

proportional to the material that can condense into grains) and that the luminosity of OH138 near maximum light is also in the range 55000–80000 $L_{\odot}$, then we find a ratio of the mass-loss rates of 4 : 3 : 1. This suggests that the mass-loss rate in AGB stars increases with metallicity. This is the first time that the relation between mass loss and metallicity is quantified for AGB stars.

Although we present the first detections of silicate dust features in AGB stars outside of our Galaxy, these observations also reveal the limitations of present-day ground-based observations. Even on a 4 m class telescope the limiting flux-density for which useful spectra can be obtained during summer on the southern hemisphere limits the usefulness to only the very brightest AGB stars in the MCs. In the near future the ISO mission will provide useful spectra for selected AGB stars in the MCs. For an order of magnitude improvement in ground-based observations from the southern hemisphere one likely has to wait for MIIS (Mid-Infrared Imager/Spectrometer) on the VLT (Moorwood 1994) to be commissioned.

The observing trip of M.G. to the Anglo-Australian Telescope and his subsequent stay at ADFA were made possible by financial support from the Franco-Australian fund for scientific collaboration.

REFERENCES

Aitken, D. A., & Roche, P. F. 1982, MNRAS, 200, 217
Blanco, V. M., & McCarthy, M. F. 1991, AJ, 100, 674
Blanco, V. M., McCarthy, M. F., & Blanco, B. M. 1980, ApJ, 242, 938
Burstein, D., & Heiless, C. 1982, AJ, 87, 1165
David, P., & Papoular, R. 1990, A&A, 237, 425
Fluks, M. A., Plez, B., Thé, P. S., de Winter, D., Steenman, H. C., & Westerlund, B. E. 1994, A&AS, 105, 311
Groenewegen, M. A. T. 1993, Ph.D. thesis, Univ. of Amsterdam
Herman, J., & Habing, H. J. 1985, A&AS, 59, 523
Hughes, S. M. G. 1989, AJ, 97, 1634
Jiang, B.-W., & Hu, J.-Y. 1992, Chinese Astron. Astrophys., 16, 416
Jones, T. W., & Merrill, K. M. 1976, ApJ, 209, 509
Jura, M. 1986, ApJ, 303, 327
Moorwood, A. F. M. 1994, in Infrared Astronomy with Arrays: the Next Generation, ed. I. S. McLean (Dordrecht: Kluwer), 465
Neckel, Th., & Klare, G. 1980, A&AS, 42, 251
Noguchi, K., Qian, Z., Wang, G., & Wang, J. 1993, PASJ, 45, 65
Payne-Gaposhkin, C. H. 1971, Smithsonian Contrib. Astrophys., 13, 1
Rebeirot, E., Azzopardi, M., & Westerlund, B. E. 1991, A&AS, 97, 603
Reid, N. 1991, ApJ, 382, 143
Reid, N., Mould, J., & Thompson, I. 1987, ApJ, 323, 433
Reid, N., Tinney, C., & Mould, J. 1990, ApJ, 348, 98
Schutte, W. A., & Tielens, A. G. G. M. 1989, ApJ, 343, 369
Schwering, P. B. W., & Israel, F. P. 1989, A&AS, 79, 79
Smith, R. G., & Herman, J. 1990, A&A, 227, 147
van Langevelde, H. J., van der Heiden, R., & Schooneveld, C. 1990, A&A, 239, 193
Volk, K., & Kwok, S. 1988, ApJ, 331, 435
Wesselius, P. R., de Jonge, A. R. W., Kester, D. J. M., & Roelfsema, P. R. 1992, in Infrared Astronomy with ISO, ed. T. Encrenaz & M. F. Kessler (New York: Nova), 509
Wood, P. R., Bessell, M. S., & Fox, M. W. 1983, ApJ, 272, 99
Wood, P. R., Moore, G. M., & Bessell, M. S. 1995, in preparation (W95)
Wood, P. R., Whiteoak, J. B., Hughes, S. M. G., Bessell, M. S., Gardener, F. F., & Hyland, A. R. 1992, ApJ, 397, 552 (W92)
Zijlstra, A. A., Loup, C., Waters, L. B. F. M., Whitelock, P. A., & Guglielmo, F. 1995, A&A, submitted